

## Multiferroic properties of ferromagnetic and ferroelectric coupled Mn-Zn ferrite-BaTiO<sub>3</sub> composite

Atiya Farheen, Thirupathi Gadipelly & Rajender Singh

To cite this article: Atiya Farheen, Thirupathi Gadipelly & Rajender Singh (2017) Multiferroic properties of ferromagnetic and ferroelectric coupled Mn-Zn ferrite-BaTiO<sub>3</sub> composite, *Ferroelectrics*, 516:1, 82-89, DOI: [10.1080/00150193.2017.1362287](https://doi.org/10.1080/00150193.2017.1362287)

To link to this article: <https://doi.org/10.1080/00150193.2017.1362287>



Published online: 07 Nov 2017.



Submit your article to this journal [↗](#)



Article views: 28



View related articles [↗](#)



View Crossmark data [↗](#)



# Multiferroic properties of ferromagnetic and ferroelectric coupled Mn-Zn ferrite-BaTiO<sub>3</sub> composite

Atiya Farheen, Thirupathi Gadipelly, and Rajender Singh

School of Physics, University of Hyderabad, Hyderabad, India

## ABSTRACT

The magneto-dielectric properties can be tuned through ferromagnetic-ferroelectric composites with different Mn<sub>0.9</sub>Zn<sub>0.1</sub>FeO<sub>4</sub> to BaTiO<sub>3</sub> ratio. The two phenomena can couple and interact with each other when they exist simultaneously due to induced electric polarization in the magnetic order. The composites were synthesized using the nanoparticles of Mn<sub>0.9</sub>Zn<sub>0.1</sub>Fe<sub>2</sub>O<sub>4</sub> and BaTiO<sub>3</sub> with different composition by sintering at 1000°C. The X-ray diffraction confirms the coexistence of ferromagnetic and ferroelectric phases. The surface micrographs show variations in the porosity along with two types of inter grain connectivity. The magnetic and ferroelectric hysteresis loops confirm the magneto-electric coupling presents in the composites.

## ARTICLE HISTORY

Received 7 November 2016  
Accepted 6 June 2017

## KEYWORDS

Ferroelectric; composites; ferromagnetic; dielectric constant

## 1. Introduction

The simultaneous existence of ferroelectricity and magnetic ordering in multiferroic materials are gaining special interest due to their promising applications in various multifunctional devices. In general, combination of both ferroelectric (FE) and ferromagnetic (FM) may lead to novel functionalities which are not present in either state alone. For instance, the magnetic properties are governed by electric fields rather than magnetic field, is an excellent feature provided by multiferroic materials. The composites are essential for the development of magneto-electronic devices in different frequency regions [1–2]. Moreover, the single phase multiferroic systems are rare in nature which leads to the preparation of FM-FE composite materials [3]. The presence of magneto-electric behavior is mainly due to the magnetic-mechanical-electric interaction in FM-FE region. As a result, the shape of ferrite particles changes in the external magnetic field due to the magnetostrictive effect and the produced strain passes to the piezoelectric phase. This will appear as the variation in the electric polarization. Therefore, the composites with high magnetostriction and piezoelectric coefficient are responsible for producing high magneto-electric coupling [4–6]. Hence, the Mn<sub>0.9</sub>Zn<sub>0.1</sub>Fe<sub>2</sub>O<sub>4</sub> (MZF) and BaTiO<sub>3</sub> (BT) are chosen for the FM-FE composites because of their good magnetostriction and piezoelectric properties [7–8], respectively. Further, the magnetic properties of these composites will aim the control over the ferroelectric properties in the magnetic field.

**CONTACT** Rajender Singh  [rsinghsp@gmail.com](mailto:rsinghsp@gmail.com)

Color versions of one or more of the figures in the article can be found online at [www.tandfonline.com/gfer](http://www.tandfonline.com/gfer).

© 2017 Taylor & Francis Group, LLC

In the present work, our attention was given to the effect of MZF on BT involving study of magnetic and electric properties to confirm the multiferroic behavior of the FM-FE composites and to find the FM and FE ordering in the FM-FE composites. The magnetic and electric properties can be tuned by changing FE ion content in the composites.

## 2. Experimental

The composites were synthesized using the nanoparticles of  $\text{Mn}_{0.9}\text{Zn}_{0.1}\text{Fe}_2\text{O}_4$  (MZF) and  $\text{BaTiO}_3$  (BT) with BT to MZF ratio of 37:63, 50:50 and 75:25 by sintering at  $1000^\circ\text{C}$  for 6 hours. The optimized composition of MZF nanoparticles ( $\text{Mn}_{0.9}\text{Zn}_{0.1}\text{Fe}_2\text{O}_4$ ) were synthesized using co-precipitation method as mentioned in our earlier work [8]. While, the BT nanoparticles were synthesized by hydrothermal method. The stoichiometric amount of  $\text{Ba}(\text{OH})_2 \cdot 8\text{H}_2\text{O}$  and  $\text{TiO}_2$  were mixed in deionized water. Further, the NaOH was added to the solution according to metal ions to hydroxide ions ratio 3:5 for holding the Ti-ion (FE) state. The solution was sealed in an autoclave and heated at  $200^\circ\text{C}$  for 10h. The excess NaOH was removed with deionized water until the pH reached 7, and then dried at  $100^\circ\text{C}$  [9]. Finally, the synthesized compositions were used for the preparation of FM-FE composites in solid-state reaction method. Micrographs were recorded using Field Emission Scanning Electron Microscopy (FESEM) CARL-ZEISS ULTRA 55. The XRD patterns were recorded using Bruker (Advanced D8) diffractometer equipped with  $\text{Cu-K}\alpha$  source. The magnetization plots were carried out using a Quantum Design PPMS-VSM. The disc shaped pellets were coated with silver paste for making electrodes. The dielectric constant measurements were carried out using Agilent E4980A LCR meter at 300K in the frequency range from 20Hz to 2MHz. The ferroelectric hysteresis measurements were carried out using Radiant PE-loop tracer at room temperature.

## 3. Results and discussion

The crystal structure of MZF and BT nanoparticles are cubic spinel and tetragonal respectively confirmed from X-ray diffraction analysis as reported in literature [8–9]. Figure 1 shows the XRD pattern of FM-FE composites with different compositions. According to the Joint Committee on Powder Diffraction Spectra (JCPDS), the diffraction peaks evidenced in Figure 1 are related to the crystal structure of MZF – BT, which confirms the simultaneous existence of FE (indexed with “○”) and FM (indexed with “\*”) phases. It is observed that BT (tetragonal) is formed as major phase.

Figure 2 shows the FESEM micrographs of FM-FE composites with variation of BT-content 37, 50 and 75%. The variation of porosity and grain size is observed for the different FM-FE composites. Moreover, the microstructure changes from large to small sized grains when BT content increases. This is attributed to a decrease in apparent density of the system with addition of BT in MZF. It is observed from the micrographs that the composite system consists of two kinds of regions: one corresponds to FM and the other corresponds to FE phase. We also observed mixed phase grain boundaries in FM-FE composites from micrographs.

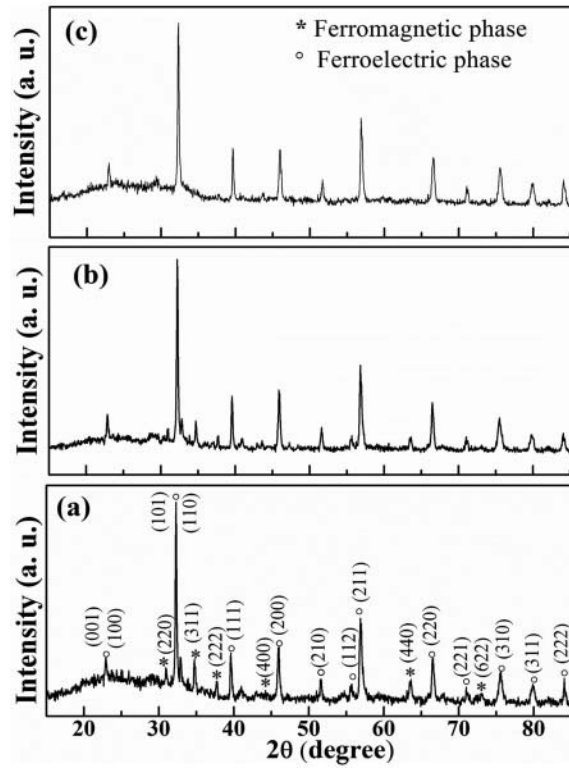


**Figure 1.** XRD pattern of FM-FE composites of different Ti to Fe ratio respectively.

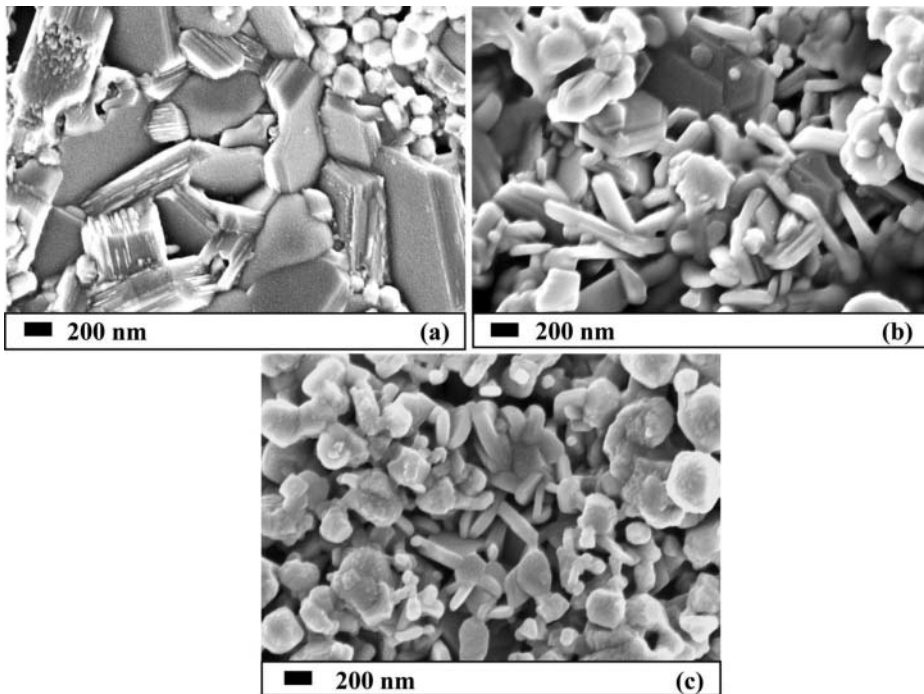


**Figure 2.** FESEM micrographs of FM-FE composites of different Ti to Fe ions ratio respectively.

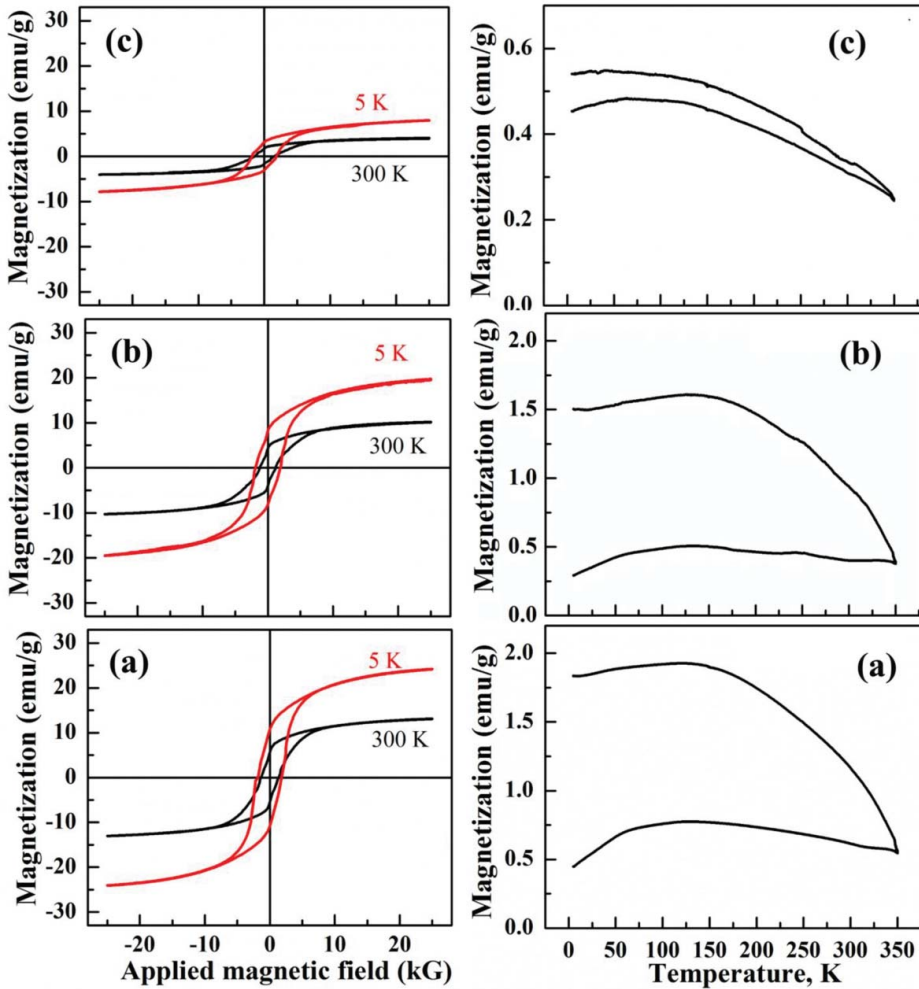


**Figure 3.** The  $M(H)$  and  $M(T)$  plots (from left to right) of FM-FE composites with different Ti to Fe ions ratio respectively.

Figure 3 (left) shows the magnetization ( $M(H)$ ) plots of the FM-FE composites at 300 and 5K with variation of 37, 50 and 75% BT-content. The increase in coercivity and decrease in magnetization is observed in the  $M(H)$  plots at 300 and 5K with the inclusion of BT-content. This indicates the existence of non-magnetic ferroelectric phase with ferrite phase. The  $M(H)$  plot of pure MZF shows the soft ferrimagnetic nature with high magnetic moment as reported in our earlier work [8]. The soft ferrimagnetic nature in FM-FE composites is reduced due to the suppression of MZF spinel ferrite phase with inclusion of non-magnetic FE phase as supported by XRD data analysis. The magnetic particles are separated by ferroelectric particles, which influences the magnetic coupling among the magnetic particles. The magnetization ( $M(T)$ ) plots were recorded from 5 to 350K in zero field cooled (ZFC) and field cooled (FC) mode (Figure. 3, right). The  $M(T)$  plot of MZF show long range FM order. We observed significant changes in  $M(T)$  plots when we include FE ions in FM ordered system. And the long range order is decreased due to the FM-FE coupling in the composites.

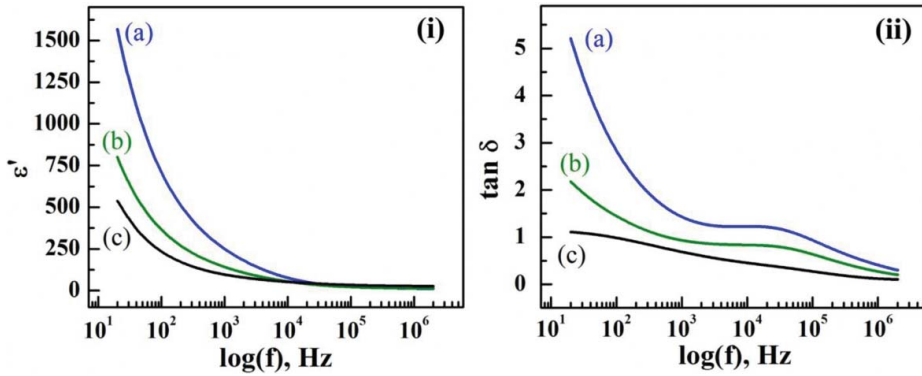


**Figure 4.** The frequency ( $f$ ) dependent dielectric constant ( $\epsilon$ ) and loss ( $\tan \delta$ ) of the FE-FM composites (a), (b) and (c) sintered at  $1000^\circ\text{C}$  respectively.

The magnetization decreases as indicated by  $M(T)$  plots with increasing BT-content. This indicates the tunability of magnetic properties by changing FE ion content in the FE-FM composites [10–15].

The variations of the dielectric constant ( $\epsilon$ ) and dielectric loss ( $\tan \delta$ ) of FM-FE composites in the frequency range from 10 Hz to 1 MHz at room temperature are shown in Figure 4 (i) and (ii), respectively. It is observed that the dielectric constant and loss values decrease with increasing frequency, until it reaches saturation value around 10 KHz. The variation of dielectric constant with frequency is due to the fact that the electric dipoles are unable to follow the alternate electric field oscillations under higher frequencies. At low frequencies, dielectric constant is found to have higher values due to the presence of heterogeneity in the FM-FE composites, which gives rise to space charge polarization and interface polarization. Since, in the FM-FE composites the ferroelectric grains are surrounded by the ferrite grains or vice versa, the FE-FM distribution makes two types of inter grain connectivity which imply two types of ionic relaxations in the low frequency region confirming the results from FESEM micrographs. Two dielectric relaxations are observed in the frequency ( $f$ ) dependent dielectric constant ( $\epsilon$ ) and loss ( $\tan \delta$ ) of the samples corresponding to the FESEM micrographs. The FM-FE composites show high values of dielectric constant ( $\epsilon$ ) and dielectric loss ( $\tan \delta$ ) with an increase in ferrite content (MZF). The impurities and imperfections present in the system cause the polarization lag with the applied field. Apart from this, the density (porosity) of the composites is also a key factor which will affect the dielectric constant and loss [16–18].

Figure 5 shows the ferroelectric hysteresis data at room temperature for FM-FE composites as a function of composition. The P-E loop of the composite shows rounded tips instead of typical hysteresis loops, indicating high leakage. The reduction in saturation polarization is due to the porosity present in the system with increasing BT-content. Generally, the ferroelectric properties of the composites can be explained with domain size, structure and wall movement. The coupling between ferromagnetic and ferroelectric ordering will cause the magneto-electric coupling which gives the interesting multiferroic property [19]. Moreover, the ferrite domains are bigger than the ferroelectric domains which causes strong magneto-electric coupling at the domain walls. When the BT-content is increased in the composites, the decrease in coercivity ( $E_c$ ) and saturation field ( $E_s$ ) is

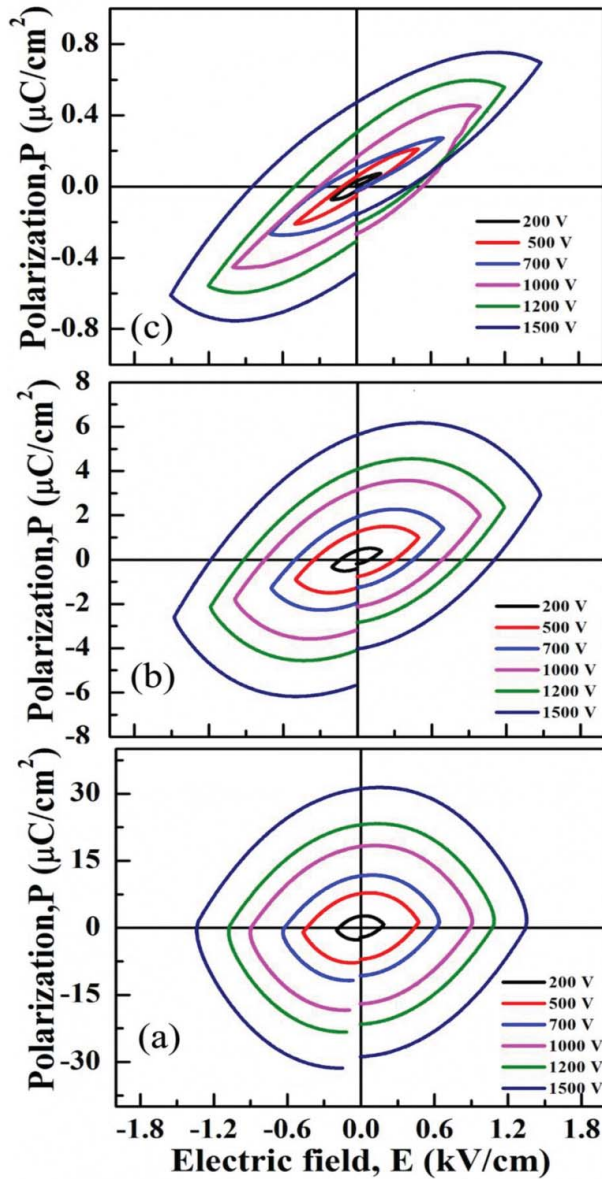


**Figure 5.** The polarization vs. electric field plots of the FE-FM composites of different composition sintered at 1000°C.

observed. Generally, the coercive field is related to grain connectivity or diffusivity at the grain boundaries which depends on the relative theoretical density. In this case, the composition of composite (different FM-FE matrix) will affect not only the relative density but also the distance between the ferroelectric ions (poles). This will alter the interaction between the internal poles in the composite because ferroelectric region is surrounded by ferrite region. So the change in the coercivity is observed with BT-content variation. The decrease in saturation polarization is due to porosity in the BT-rich compositions which is supported by FESEM micrograph analysis [18–19].

## 4. Conclusion

The (MZF – BT) composites were synthesized using  $\text{Mn}_{0.9}\text{Zn}_{0.1}\text{Fe}_2\text{O}_4$  and  $\text{BaTiO}_3$  nanoparticles with BT to MZF ratio of 37:63, 50:50 and 75:25 by sintering at  $1000^\circ\text{C}$ . The XRD pattern confirms the coexistence of FM and FE phases. The FESEM micrographs show two types of grains with varying porosity. The variation of magnetic field dependent ( $M(H)$ ) and thermomagnetic  $M(T)$  properties, ferroelectric hysteresis loops and dielectric properties indicate the coexistence of FM-FE coupling. The formation of FM and FE phases are confirmed using structural, magnetization and electrical studies. The study directs the magnetic field controlled ferroelectric properties in the FM-FE coupled regions of the composites.

## Acknowledgment

Atiya Farheen would like to thank DST for providing INSPIRE fellowship.

## References

1. C. W. Nan, M. I. Bichurin, S. Dong, D. Viehland, and G. Srinivasan, Multiferroic Magnetolectric Composites: Historical perspective, status, and future directions, *J. Appl. Phys.* **103**, 031101 (2008).
2. S. A. Lokare, D. R. Patil, R. S. Devan, S. S. Chougule, Y. D. Kolekar, and B. K. Chougule, Electrical Conduction, Dielectric Behavior and Magnetolectric Effect in  $(x)\text{BaTiO}_3 + (1-x)\text{Ni}_{0.94}\text{Co}_{0.01}\text{Mn}_{0.05}\text{Fe}_2\text{O}_4$  ME composites, *Mater. Res. Bull.* **43**, 326–332 (2008).
3. N. A. Hill, Why Are There so Few Magnetic Ferroelectrics?, *J. Phys. Chem. B* **104**, 6694–6709 (2000).
4. J. Ma, J. Hu, Z. Li, and C. W. Nan, Recent Progress in Multiferroic Magnetolectric Composites: from Bulk to Thin Films, *Adv. Mater.* **23**, 1062–1087 (2011).
5. S. Priya, R. Islam, S. Dong, and D. Viehland, Recent Advancements in Magnetolectric Particulate and Laminate Composites, *J. Electroceram.* **19**, 147–164 (2007).
6. R. W. McCallum, K. W. Dennis, D. C. Jiles, J. E. Snyder, and Y. H. Chen, Composite Magnetostrictive Materials for Advanced Automotive MagnetoMechanical Sensors, *Low Temp. Phys.* **27**, 266 (2001).
7. J. Zhu, C. Jin, W. Cao, and X. Wang, Phase Transition and Dielectric Properties of Nanograin  $\text{BaTiO}_3$  Ceramic Under High Pressure, *Appl. Phys. Lett.* **92**, 242901 (2008).
8. G. Thirupathi, and R. Singh, Crystal Structure and Magnetic Properties of Mn-Doped Zn-Ferrite Nanoparticles, *IEEE trans. magn.* **50**, 11 (2014).
9. S. K. Tripathy, T. Sahoo, M. Mohapatra, S. Anand, and R. P. Das, XRD studies on hydrothermally synthesized  $\text{BaTiO}_3$  from  $\text{TiO}_2\text{--Ba(OH)}_2\text{--NH}_3$  system, *Mater. Lett.* **59**, 3543 (2005).
10. M. Rawat, and K. L. Yadav, Dielectric, ferroelectric and magnetolectric response in  $\text{Ba}_{0.92}(\text{Bi}_{0.5}\text{Na}_{0.5})_{0.08}\text{TiO}_3\text{--Ni}_{0.65}\text{Zn}_{0.35}\text{Fe}_2\text{O}_4$  composite ceramics, *Smart Mater. Struct.* **23**, 085032 (10pp) (2014).
11. R. S. Devan, and B. K. Chougule, Magnetic properties and dielectric behavior in ferrite/ferroelectric particulate composites, *Physica B* **393**, 161–166 (2007).
12. U. Acevedo, T. Gaudisson, R. O. Zempoalteca, S. Nowak, S. Ammar, and R. Valenzuela, Magnetic properties of ferrite-titanate nanostructured composites synthesized by the polyol method and consolidated by spark plasma sintering, *J. App. Phys.* **113**, 17B519 (2013).
13. Y. Liu, Y. Wu, D. Li, Y. Zhang, J. Zhang, and J. Yang, A study of structural, ferroelectric, ferromagnetic, dielectric properties of  $\text{NiFe}_2\text{O}_4\text{--BaTiO}_3$  multiferroic composites, *J. Mater. Sci.: Mater. Electron.* **24**, 1900–1904 (2013).
14. J. Shen, Y. Bai, J. Zhou, and L. Li, Magnetic Properties of a Novel Ceramic Ferroelectric–Ferromagnetic Composite, *J. Am. Ceram. Soc.* **88**, 3440–3443 (2005).



15. G. Thirupathi, and R. Singh, Structural and FMR lineshape analysis of Mn Zn-ferrite nanoparticles, *AIP Conf. Proc.* **1665**, 050133 (2015).
16. M. A Ahmed, S. T. Bishay, and G. Abdelatif, Effect of ytterbium on the electrical properties of Li-Co ferrite, *J. Phys. Chem. Solids* **62**, 1039–46 (2001).
17. C. G. Koops, On the Dispersion of Resistivity and Dielectric Constant of Some Semiconductors at Audiofrequencies, *Phys. Rev.* **83**, 121–4 (1951).
18. X. Xu, Z. Wu, Y. Jia, W. Li, Y. Liu, Y. Zhang, and A. Xue, Multiferroic Properties of Nanopowder-Synthesized Ferroelectric-Ferromagnetic  $0.6\text{BaTiO}_3\text{-}0.4\text{NiFe}_2\text{O}_4$  Ceramic, *J. Nanomater.* **2015**, 613565 (2015).
19. G. Catalan, H. Bea, S. Fusil, M. Bibes, P. Paruch, A. Barthelemy, and J. F. Scott, Fractal Dimension and Size Scaling of Domains in Thin Films of Multiferroic  $\text{BiFeO}_3$ , *Phys. Rev. Lett.* **100**, 027602 (2008).